ISIJ International, Vol. 55 (2015), No. 7, pp. 1353–1360

# Low Computational-complexity Model of EAF Arc-heat Distribution

Amirhossein FATHI,[1)] Yadollah SABOOHI,[2)] Igor ŠKRJANC[3)] and Vito LOGAR[3)]*

1) Department of Energy Engineering, Sharif University of Technology, Azadi Ave., Tehran, 11365-9567 Iran.
2) Sharif Energy Research Institute (SERI), Sharif University of Technology, Azadi Ave., Tehran, 11365-9567 Iran.
3) Laboratory of Modelling, Simulation and Control, Faculty of Electrical Engineering, University of Ljubljana, Tržaška 25, SI-1000 Ljubljana, Slovenia.

(*Received on February 9, 2015; accepted on March 24, 2015*)

The paper presents a computational model and the corresponding algorithm for estimating the arc energy distribution to conductive, convective and radiative heat transfer in an electric arc furnace (EAF). The proposed algorithm uses channel arc model (CAM) in order to compute the distribution of the arc energy through empirical equations (to approximate arc radius), ideal gas law (to approximate arc density) and results of magneto-hydro-dynamic (MHD) models (to approximate arc pressure, temperature and velocity). Results obtained using the proposed algorithm are comparable with other similar studies; however, in contrast to other arc-energy distribution models, this model requires only two input variables (arc length and arc current) in order to calculate the energy distribution. Furthermore, simple algebraic equations used in the algorithm ensure minimal computational load and consequently lead to short calculation times which are approximately one hundred thousand (100 000) times smaller than solving the MHD model equations, making the algorithm suitable for real-time applications, such as smart monitoring and model-based control. The algorithm has been validated by two different approaches. First, the simulation results have been compared to a study dealing with arc-heat distribution in plasma arc furnace; and second, the proposed arc module has been integrated into the frame of a comprehensive EAF model in order to estimate the EAF temperature levels and compare them with operational EAF measurements. Both validations show high levels of similarity with the comparing data.

KEY WORDS: arc current; arc heat distribution; arc length; channel arc model; EAF.

## 1. Introduction

A remarkable share of the total steel production is carried out using electric arc furnaces (EAFs), *i.e.* about 29.2% in 2011.[1)] Observing the minimum theoretical and the actual energy consumption, a noticeable gap between them can be observed. For example, theoretical minimum and the actual energy consumptions for scrap (0.1%C, 0.2%Si), with slag quality (% FeO = 25%, $CaO/SiO_2$ = 2.5) and tap temperature 1 873 K are 358 kWh/ton and 580–670 kWh/ton, respectively.[2)] Reduction in the cost of the energy transferred to molten bath is an important factor for increasing the economic productivity in steel industry. This goal can be achieved if the slag height and arc lengths are coordinated with technical and economical indexes of the EAF. Slag height has a direct effect on the heat transferred to the walls, heat absorbed from the arcs and energy absorbed or released by chemical reactions. Also, slag height influences the operational costs as the arc length and arc current have a direct effect on energy released from the arc. Since electric arcs are the main source of energy in electric arc furnaces, the electric energy provided by them represents approximately 75–85% of the total energy in low to medium power furnaces and approximately 50–60% of the total energy in ultra-high power furnaces (UHP).[3)] Implementing an accurate arc module in a comprehensive model-based EAF control, which ensures optimal control of arc length and slag height can lead to substantial energy saving and associated cost reduction. If a total energy reduction in a 200 ton UHP EAF with approximate annual production of 675 000 tones is 50 kWh/ton, with an assumption of 25 kWh/ton being the electrical energy, with the price of 10 $Cent/kWh, total annual energy savings will be equivalent to 1.7 million $ per year.

It is known that the heat generated by the arcs is dissipated into the furnace by all three mechanisms of heat transfer (convection, conduction and radiation); however, the amount of the heat, transferred by each mechanism varies according to several factors, such as arc length, arc current, slag height, stage of melting *etc.* Development of a computational model of the arc, which allows estimation of the arc-heat distribution should therefore include all three types of heat transfer mechanisms, which can also be used to obtain the overall energy balance of the EAF. Application of such models may provide appropriate tools for optimizing the energy flow or use of model-based control systems in the EAFs.

* Corresponding author: E-mail: vito.logar@fe.uni-lj.si
DOI: http://dx.doi.org/10.2355/isijinternational.55.1353

Many models have been developed to simulate electrical arcs among which the MHD model,[4,5] Cassie-Mayr model,[6] channel arc model (CAM)[7] could be mentioned as examples. MHD models are more comprehensive than other types and include calculation of arc velocity profile, pressure profile and temperature profile;[4] however, the flaw of such models is that their parameterization and implementation require a large number of experimental data.[6] On the other hand, Cassie-Mayr arc models are easier to parameterize and they could be integrated into broader EAF models; but, they are usually used to model low arc powers.[6] Such models are not appropriate for obtaining the distribution of the dissipated heat attributed to different mechanisms of the heat transfer. The most appropriate model for estimating the distribution related to each heat transfer mechanism is the CAM model, which was used by Sanchez *et al.*[7] in order to determine the share of each heat transfer mechanism in different gas plasma. Although CAM models deliver extensive information, they rarely provide efficient and instantaneous solution for analysis of model parameters and input variables, such as arc length, arc temperature, arc density and especially arc radiation density. Hence, such model can hardly be used for online smart monitoring or control oriented purposes. Therefore, further development of CAM models may be envisaged as a complementary step for enhancing the applicability of mathematical models in industrial application.

The present research work is related to further development of a comprehensive EAF model, which ensures efficient implementation of the arc model. The model is based on the actual physics in an EAF and allows appropriate arc length and arc current calculation, which represent the inputs to the CAM model. The enhancement of the EAF model with the presented arc-heat distribution module leads to greater accuracy of the calculations and promotes their use in model-based control applications in order to obtain optimum arc lengths and slag height. Development of the EAF model-based control represents a future goal with the highest priority. For this reason an accurate process model, able to provide calculations with minimum information and low computational complexity is required.

A literature review of the existent EAF models[8–20] indicates a lack of accurate arc models that could be applied for smart sensing, control or optimization of the energy flows. It is assumed that such model should present specific features that support their industrial application, including minimum input requirement, sufficient accuracy, simple mathematics and short calculation times.

Mathematical EAF models can be categorized into 2 groups, *i.e.* partial models, which are used for studying particular phenomena in the EAF and comprehensive models, which more or less represent all major mechanisms in the EAF. The first group can be divided into 2 sub-groups. The first sub-group involves models, such as: EAF electrode control, arc flicker impacts, investigation of the EAF effects on the electrical grids, *etc.*[8,10–12] In this group, arc behavior is simulated by equations describing the relations between the voltage and the current[10–12] and passive devices.[8] Each stage of the melting process can be modeled in a particular way. The arc modules used in these models have not been developed to compute arc energy dissipation. The second sub-group involves the models that have been developed to estimate arc shape evolution, heat transfer, molten velocity, *etc.*[4,5,7] The arc modules used in these models are based on MHD models or CAM.[4,7] Despite of heavy computational cost, the results may not be comparable to the actual EAF situation, neither to other similar studies. For instance, Sanchez *et al.*[7] tried to obtain the share of heat transfer mechanisms for different gas atmospheres in an EAF. A CAM model was used to predict the share of each heat transfer mechanism. The share of convective heat transfer when air is employed to form plasma in an EAF was predicted at 72.5%, which is more than the expected value.[20,21]

The second group involves models, which describe all significant parts of the EAF process;[13–20] however, those models hardly consider arc energy dissipation, except Logar *et al.*,[18,19] who assumed constant values for arc energy distribution (*i.e.* 20% convective heat, 75% radiation heat, 2.5% of the energy transferred to gas zone and 2.5% of the energy lost to electrodes) and Ghobara[20] who as well as Logar *et al.*[18,19] considered constant coefficients for the heat transferred from the arc. Therefore, these EAF models are not appropriate for estimating optimum inputs. Hence, further development of EAF models is required, which could ensure more accurate calculation of the heat distribution and it may also provide information on the arc current and arc length.

The arc model and the corresponding algorithm proposed in the present paper are designed to have sufficient accuracy, low computational load and can easily be integrated into broader EAF models in contrast to MHD models, which are based on partial differential equations and require a considerable input and process information. Such a conceptual development allows a design of smart monitoring, model-based control and optimization systems. As shown in **Fig. 1**, the arc model can be implemented to an EAF model as an arc module. In simulation applications, the arc current is known (input) and the arc length can be obtained from the arc current, arc power and arc voltage. In control applications, the arc length can be estimated similarly as in simulation applications, followed by the calculation of optimum arc current and arc length. Afterwards, optimal electrode positions can be obtained using previous calculations and current bath height.

## 2. Modelling

The present section describes the process of modelling the electric arc and the proposed calculation algorithm. The model describes the arc with 2 input variables (arc current and arc length), 3 state variables (heat accumulation or depletion) and 5 output variables (rates of heat transfer through various mechanisms, arc voltage, and arc radius). Although the arc length is not an actual manipulated variable in an EAF, it is considered as a manipulated variable, which is explained after presentation of the algorithm.

The arc releases thermal energy $P_a$, which is dissipated by 3 mechanisms, *i.e.* electron flow $P_e$, convection $P_{conv}$, and radiation $P_r$[7,21] as denoted by Eq. (1):

$$P_a = P_r + P_e + P_{conv}. \quad \text{..... (1)}$$

The CAM, modified for EAFs, is used to compute arc

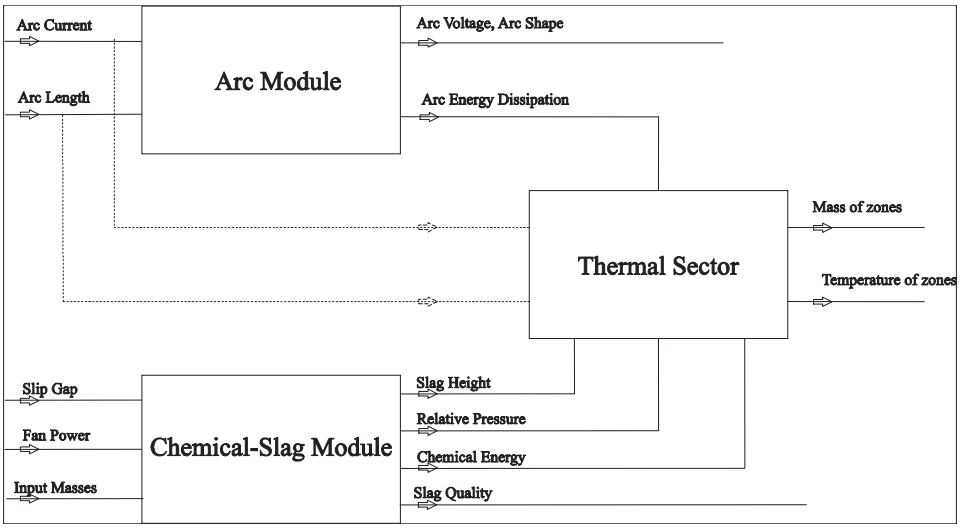


**Fig. 1.** The arc model integrated into a conceptual comprehensive EAF model.

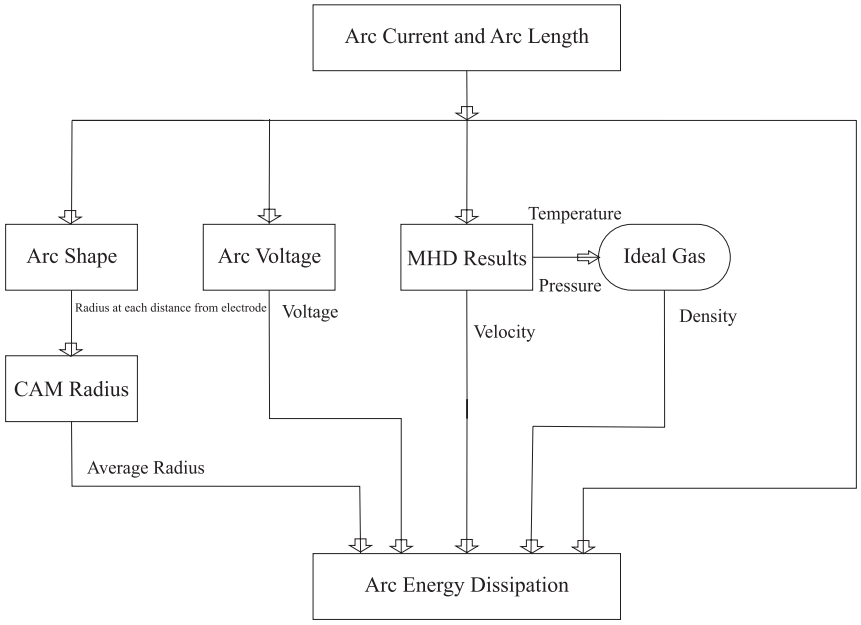


**Fig. 2.** Envisaged algorithm for approximating the arc energy distribution.

energy distribution[7] and includes the following assumptions:

- the local thermodynamic equilibrium (LTE) is assumed, meaning that electrons and positive ions are at the same temperature;[7] therefore, plasma acts as a continuous environment,[22]
- cylindrical shape is assumed for plasma arc region, even though in practice the shape of the arc is similar to cone,
- temperature and current are considered uniform over the entire plasma region.

The CAM model addresses the following types of heat transfer as a function of arc length and arc current: radiation, convection and electron flow, which are mathematically described by Eqs. (2) to (4). The electron flow contains electron condensation (first part of Eq. (3) – [$I\,O_{an}$]), Thompson Effect (second part of Eq. (3) – $\left[I\frac{5k_BT_k}{2e}\right]$) and electron acceleration in the anode fall (third part of Eq. (3) – [$I\,U_{an}$]).

$$P_r = \pi R_{arc}^2 l u, \quad \text{..... (2)}$$

$$P_e = I\left[O_{an} + \frac{5k_BT_k}{2e} + U_{an}\right], \quad \text{..... (3)}$$

$$P_{conv} = \pi R_{arc}^2 \rho_k \bar{v}_k \left(h_k - h_f\right), \quad \text{..... (4)}$$

where $P_r$ is the arc radiation power [W], $P_e$ is the arc electron flow [W], $P_{conv}$ is the arc convective power [W], $R_{arc}$ is the cylindrical arc radius [m], $l$ is the arc length [m], $u$ is the arc radiation density [W/m$^3$], $I$ is the arc current [A], $O_{an}$ is work function for the anode [V], $k_B$ is the Boltzmann constant [J/K], $T_k$ is the arc temperature [K], $e$ is the electron charge [J], $U_{an}$ is the anode voltage drop [V], $\rho_k$ is the arc density [kg/m$^3$], $\bar{v}_k$ is the average arc velocity [m/s], $h_k$ is the arc specific enthalpy [J/kg] and $h_f$ is the surrounding air specific enthalpy [J/kg].

**Figure 2** shows the proposed algorithm for approximating the distribution of the arc energy dissipation.

As it can be observed in Fig. 2, the algorithm uses several auxiliary calculation methods as a function of arc current and arc length, in order to provide necessary inputs for cal-

culating the arc energy distribution/dissipation. Those are:

- arc shape calculation: computes the arc radius at a given distance from the cathode using arc length and arc current, which is further used to approximate the voltage and the radius of the arc cylinder,
- CAM radius calculation: computes the average arc velocity to determine the dissipation of the arc energy, whereas CAM considers cylindrical shape for the arc (arc shape is transferred to a cylindrical shape),
- arc voltage calculation: computes the arc voltage using arc length (independent variable) and the arc radius (dependent variable),
- MHD results: computes the arc temperature and arc pressure that are needed to obtain the arc density and arc velocity. The later parameters are directly used to calculate the arc energy dissipation. Arc temperature and arc pressure are used to compute arc density,
- ideal gas law calculation: is utilized to compute arc density using the arc temperature and arc pressure that are estimated in the MHD block.

Advantages of the proposed algorithm over other similar approaches are the possibility of prediction of the heat transfer amount through each mechanism with only 2 input variables (arc length and arc current). In addition, it incorporates simple mathematics, being computationally efficient and sufficiently accurate in order to be integrated into EAF models as an arc module. Detailed description of sub-modules is presented in the following sections.

### 2.1. Arc Shape Calculation

Electric arc originates from a spot on the cathode and conically extends to the molten surface.[23] In order to calculate the arc voltage and the CAM radius, the arc radius at the cathode and on the molten surface need to be obtained first. The arc radius at any distance from the cathode surface can be obtained by Eq. (5):

$$\frac{r}{r_k} = 3.2 - 2.2\exp\left(-\frac{z}{5r_k}\right), \quad \text{..... (5)}$$

where $r$ represents the arc radius [m] at distance $z$ from cathode surface (electrode), $r_k$ represents the arc radius [m] at the cathode and can be obtained by $r_k = \sqrt{\frac{I}{\pi * j_k}}$, where $I$ is the arc current [A] and $j_k$ is the arc current density at the cathode [3 500 A/cm$^2$].[24]

### 2.2. CAM Radius Calculation (Arc Shape Deformation)

Transformation of the conical arc shape to cylindrical arc shape requires information of the arc cone volume, which can be obtained by Eq. (6) and is further used to calculate the CAM radius by Eq. (7):

$$Vol = \pi * \frac{l}{3}\left[r_k^2 + r_a^2 + r_a r_k\right], \quad \text{..... (6)}$$

$$R_{arc} = \sqrt{\frac{Vol}{\pi * 1}}, \quad \text{..... (7)}$$

where $r_a$ is the arc radius [m] at the anode (bath).

Sanchez *et al.*[4] reported the arc radius to be 5.96 cm at arc current of 85 kA and arc length of 45 cm. The proposed algorithm in the present work computes the arc radius to be 5.96 cm also in similar conditions.

### 2.3. Arc Voltage Calculation

Arc voltage is a function of arc current, arc length and arc density.[23,25] Using the calculated arc radiuses, the arc voltage at each distance from the cathode surface can be obtained by Eq. (8):

$$V_a = \rho_a \sqrt{\frac{Ij_k}{\pi}} \int \left(\frac{r_k}{r}\right)^2 dm, \quad \text{..... (8)}$$

$$m = \frac{z}{r_k},$$

where $\rho_a$ represents the arc resistivity [0.0175 Ω/cm].[25]

### 2.4. MHD Results

A procedure of estimating the MHD model is aimed to determine arc temperature, arc pressure and arc velocity. The average arc temperature and pressure are used to calculate the arc density and the average velocity that are needed to approximate the arc energy dissipation. The average temperature is considered to be 16 136 K[5,22] and the average pressure is assumed to be 1 200 kPa.[5] The average velocity of the arc can be obtained by Eq. (9):[7]

$$\bar{v}_{arc} = \frac{0.5I}{\pi R_{arc}} \sqrt{\frac{5}{3}\frac{u_0}{2\rho_k}\left[\frac{R_{arc}^2}{r_k^2} - 1\right]}, \quad \text{..... (9)}$$

where $\rho_k$ is the arc density [kg/m$^3$], approximated by Eq. (10), and $u_0$ is the magnetic permeability.

The arc velocity obtained by above equations is compatible with the arc velocity that has been reported by Qian *et al.*[26]

### 2.5. Assumptions of Ideal Gas Model

The arc plasma gas can be considered as air.[26,27] Although the air behavior under plasma conditions is remarkably different from the ideal gas, the ideal gas law still applies.[26,28] It is assumed that the arc behaves similar to the ideal gas. The arc density can then be obtained by Eq. (10) as follows:

$$\rho_k = \frac{PM}{RT}, \quad \text{..... (10)}$$

where $M$ represents the molar mass of gas (plasma), $P$ represents the average arc pressure, $T$ and $R$ are the average arc temperature and the gas constant respectively. The average temperature and pressure are obtained from the output data of MHD models. Since effective parameters in the arc density calculation are assumed constant, the procedure for estimating the arc density is executed only at the beginning of the arc model simulation.

Reynolds *et al.*[27] reported that the arc density would be 0.02593 kg/m$^3$, while the above procedure estimates it to be 0.02594 kg/m$^3$ at similar conditions.

### 2.6. Arc Energy Dissipation Calculation

The arc energy dissipation can be calculated according to Eqs. (11) and (12):

$$P_a = V_a I, \quad \text{..... (11)}$$

$$P_r = P_a - \left(P_{conv} + P_e\right). \quad \text{..... (12)}$$

The electron flow $P_e$ and the heat convection $P_{conv}$ can be computed directly from Eqs. (3) and (4) using the values that have been obtained from other auxiliary computation

modules. In this manner, all three types of heat transfer are defined and distribution of the arc energy to convection, conduction and radiation can be obtained.

### 2.7. Implementation of the Arc Model in Simulation and Control Applications

In practice, there is no reliable way to measure the arc length directly. Using conventionally measured values, such as voltage, current and electrical power and Eqs. (8) and (11), the arc length can be estimated. The procedure can be used in both simulation and control oriented applications. In simulation studies, arc energy distribution can be estimated using arc length, arc current and the algorithm proposed. The calculated energy distribution, together with arc current and arc length can then be utilized by the reference energy system (RES) in order to estimate the mass and temperature transfers. Similarly, in control applications, the arc length is computed according to the given procedure, followed by the calculation of both optimum arc lengths and other manipulated variables subject to constraints. The results can then be used to determine optimal electrode positions.

## 3. Results and Discussion

This section is devoted to presentation of the arc-energy distribution simulation results and the validation of the module developed in the present research work by two different approaches.

The model results of the arc energy dissipation in an EAF are shown in **Figs. 3** to **6**. It can be observed that results of the proposed algorithm are comparable to constant values of arc energy distribution reported by Logar *et al.*[18] and Ghobara[20] at comparable input conditions.

The relationship between the arc length, arc current and the calculated arc power is shown in Fig. 3, for different values of arc lengths (*i.e.* 10 to 60 cm) and arc currents in the range of 1 to 40 kA.

The entire region shown in Fig. 3 is not feasible, since the arc resistance must be in the feasible range,[7] which is not achievable in the combination of long arcs – low currents and short arcs – high currents. Figures 4 to 6 show the amount of heat dissipated by each of the heat transfer mechanisms. Areas marked with white pattern show the infeasible region of the arc conditions.

As it can be observed in Fig. 4, the amount of energy transferred by the electron flow decreases with either increased arc length or increased arc current. As it was noted in Fig. 3, the increase in either arc length or arc current leads to increased arc power; however, the electron flow is actually reduced due to the arc voltage drop. It can also be seen that the percentage of the electron flow in the feasible arc region lies in the range of 3.5% to approximately 18%, with the mean value of 5.5%.

Figure 5 shows that the amount of energy transferred by radiation increases when both the arc length and the arc current are increased; however, the radiation will be reduced as arc current is decreased and arc length is kept constant. Such a phenomenon is due to higher dependency of the convec-

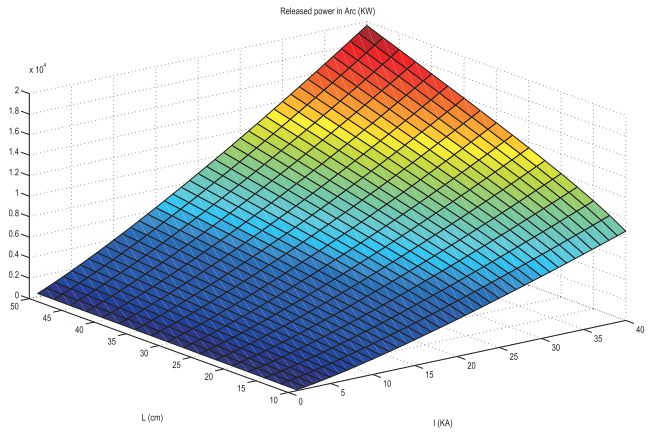


**Fig. 3.** Relation between the arc length, arc current and arc power.

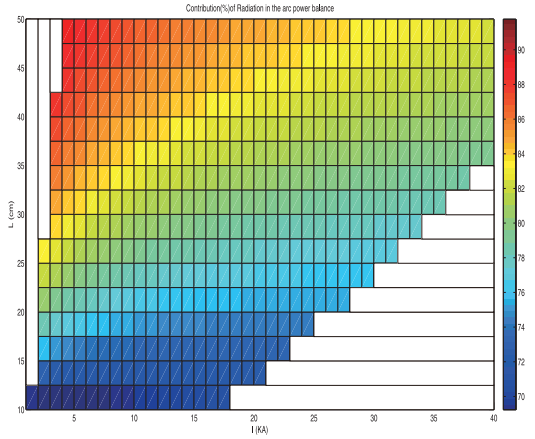


**Fig. 5.** The share of heat (in %) dissipated by the arc radiation.

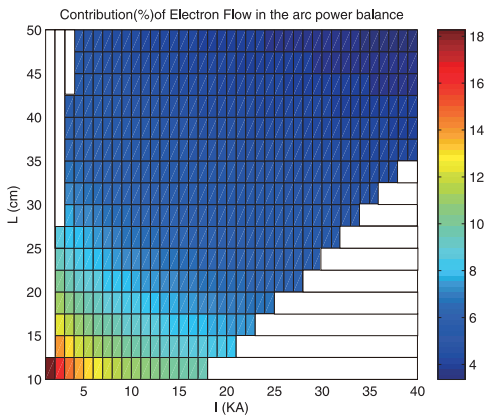


**Fig. 4.** The share of heat (in %) dissipated by the arc electron flow.

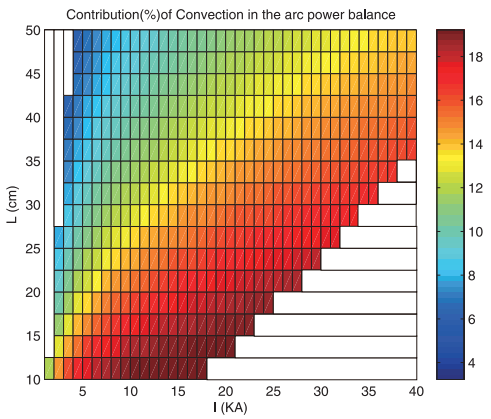


**Fig. 6.** The share of heat (in %) dissipated by the arc convection.

tion mechanism on the arc current, which can be observed in Fig. 6. The share of the radiation in the feasible region is in the range of 69% to approximately 89%, with the mean value of 80.2%.

Since the convection mechanism has a direct relation to the arc current and arc length, an increase in either the arc current or the arc length would lead to increased convective heat transfer. The share of the convection in the feasible region would be in the range of 6% to approximately 19%, with the mean value of 14.3%.

### 3.1. Validation

The first validation of the arc module is founded on the comparison of the simulated data with the results of the Plasma Arc Furnace (PAF) model reported by Makarov *et al*.[21] Since plasma gas in PAF is different from the plasma gas in EAF, *e.g.* it has higher temperature and pressure; results of the proposed model are obtained using the PAF variables and parameters implemented in the algorithm developed in the present work. Due to the similarity of the PAF and EAF, the PAF validated results could also be applied for the EAF. The required information has been extracted from the work of Makarov *et al.*[21]

**Table 1** shows the comparison of the arc energy distribution (in %) obtained by the model proposed in the present research work and the work reported by Makarov *et al.*[21] The results show the amount of arc energy dissipated as conduction, convection and radiation for three different values of arc lengths (5 cm, 20 cm and 80 cm) and the arc current of 2 000 A. It should be noted that the results presented by Makarov *et al.*[21] assume constant heat conduction although the arc lengths vary. Hence, the total of all three energy transfer mechanisms do not add up to 100%.

**Table 1.** Comparison of the arc energy distribution in PAF obtained by the application of the proposed model and the results reported by Makarov *et al.*[21]

| | | L = 5 cm | L = 20 cm | L = 80 cm |
|---|---|---|---|---|
| Makarov's study | Radiation | 36% | 76% | 82% |
| | Convection | 60% | 28% | 16% |
| | Conduction | 2% | 2% | 2% |
| Presented model | Radiation | 22.2% | 62.4% | 88.3% |
| | Convection | 60.6% | 30.1% | 9.4% |
| | Conduction | 17.2% | 7.5% | 2.3% |

As it can be seen in Table 1 the results obtained by the proposed model and the work reported by Makarov *et al.*[21] are comparable. The main difference between the results appears due to constant conductive heat transfer in Makarov's work, which does not change by altering the arc lengths. Hence, the proposed model indicates slightly different percentage of radiated heat when it is compared to the result reported by Makarov *et al.*[21]

The second validation of the arc module is performed by integrating the module into a comprehensive EAF model[18,19] in order to obtain the EAF bath temperatures and compare them with the measured EAF operational data. The measurements were performed on a 105 ton EAF, with 85 MVA transformer. The presented validation approach is indirect as the actual values of the arc-heat distribution are practically impossible to measure in an operating EAF; however, as the arc energy contributes the largest share in the EAF energy balance, high accuracy of the arc module is needed in order to obtain accurate temperature estimations. In this manner, indirect validation of the proposed algorithm is performed, using two different melting programs presented in **Table 2** and **Fig. 7**. Table 2 presents the material addition during the melting and Fig. 7 represents the rates and times of oxygen lancing, carbon injection and arc powers.

**Figure 8** and **Table 3** show the comparison of the measured and estimated bath temperatures for two different melting scenarios.

As shown in Fig. 8 and Table 3, the estimated bath temperatures are similar to the measured endpoint bath temperatures. Observing the second measurement of the second scenario, a slightly larger deviation from the simulated value occurs, which is a consequence of the EAF sampling-point selection and non-homogenous bath, as the total energy input between the samples (2 819 s and 2 990 s) is too low in order to increase the bath temperature from 1 887 K to 1 952 K. Knowing that temperature gradients in the non-stirred EAF bath can reach up to 80–120 K, the differ-

**Table 2.** Material addition for two validation scenarios.

| | | | | | | | | | |
|---|---|---|---|---|---|---|---|---|---|
| First batch | Type | Scrap | Fat coke | Lime | Dolomite | Dust | Dolomite | Lime | Lime |
| | Injection time [s] | 0 | 0 | 0 | 0 | 0 | 658 | 709 | 761 |
| | Mass [kg] | 45 900 | 1 014 | 1 080 | 1 010 | 1 437 | 460 | 500 | 520 |
| | Type | Dolomite | Scrap | Scrap | FeMn | | | | |
| | Injection time [s] | 800 | 965 | 1 750 | 3 029 | | | | |
| | Mass [kg] | 490 | 38 279 | 18 500 | 166 | | | | |
| Second batch | Type | Scrap | Fat coke | Lime | Dolomite | Lime | Lime | Lime | Lime |
| | Injection time [s] | 0 | 0 | 0 | 0 | 694 | 745 | 786 | 826 |
| | Mass [kg] | 46 418 | 699 | 1 070 | 1 000 | 510 | 510 | 510 | 520 |
| | Type | Scrap | Dolomite | Dolomite | Dolomite | Scrap | Al | SiMn | FeSi |
| | Injection time [s] | 920 | 1 531 | 1 560 | 1 613 | 1 700 | 3 038 | 3 038 | 3 038 |
| | Mass [kg] | 36 057 | 480 | 480 | 490 | 21 993 | 131 | 1 218 | 196 |

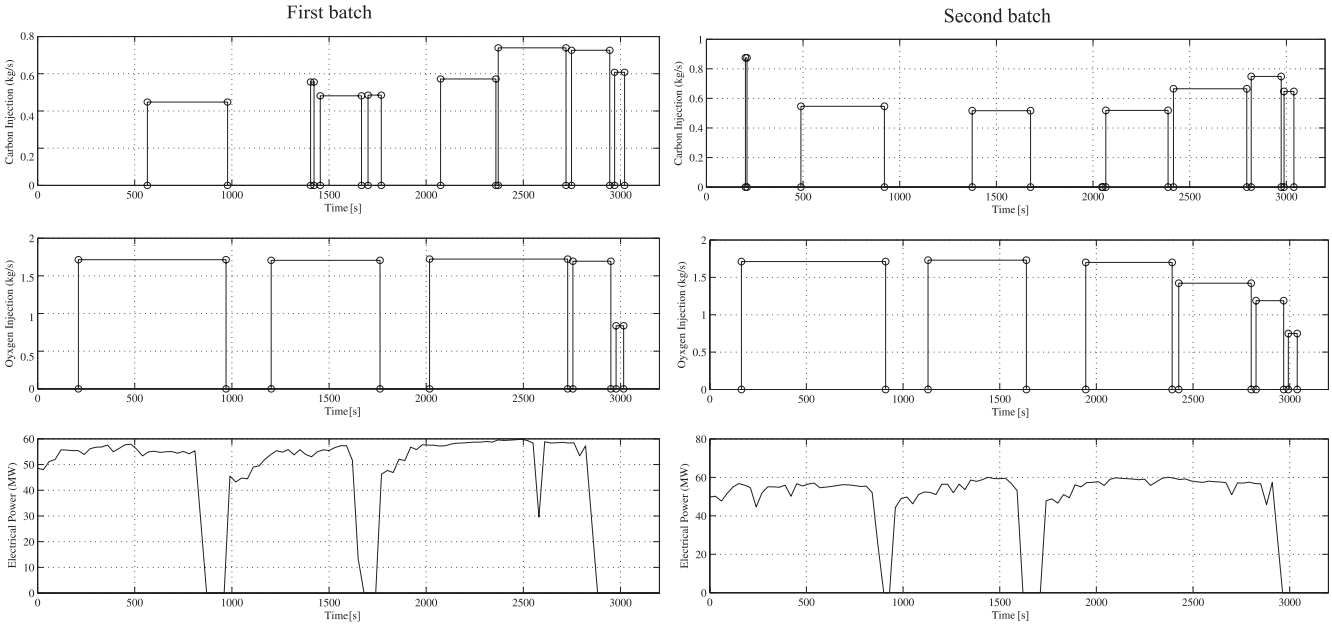


**Fig. 7.** Oxygen lancing, carbon injection and arc powers for two validation scenarios.

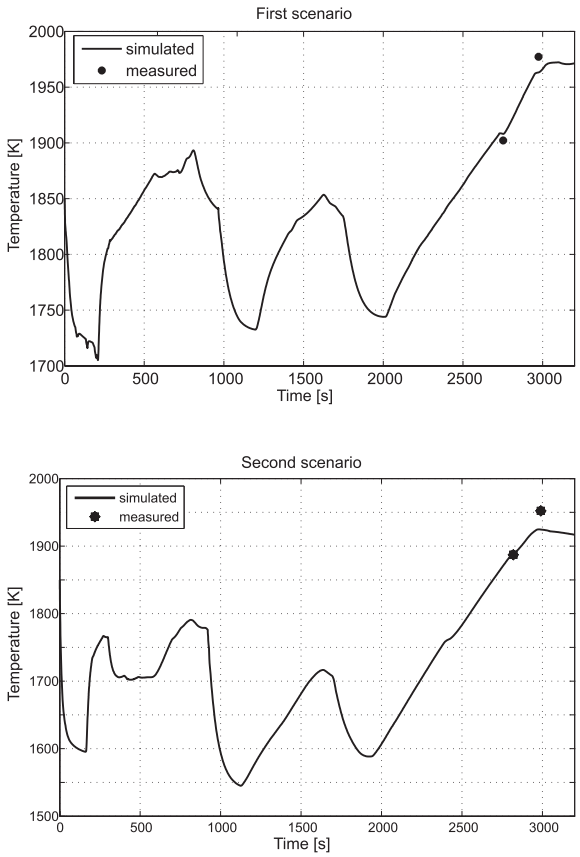


**Fig. 8.** Comparison between the measured and the simulated bath temperatures for two different melting scenarios.

ence between the measured and the simulated temperatures is acceptable. The similarity of the simulated results with the measured EAF data, especially in the prediction of the bath temperature, denotes the accuracy of the presented arc model. One of the main factors that leads to high accuracy of the model is the implementation of the arc calculation method as presented in this paper.

**Table 3.** Comparison between the measured and the simulated bath temperatures for two validation scenarios.

| | First batch | | Second batch | |
|---|---|---|---|---|
| Time [s] | 2 752 | 2 974 | 2 819 | 2 990 |
| Measured | 1 902 *K* | 1 977 *K* | 1 887 *K* | 1 952 *K* |
| Simulated | 1 908 *K* | 1 963 *K* | 1 889 *K* | 1 925 *K* |

### 3.2. Computational Demand

The proposed algorithm has been implemented in an appropriate programming language (Matlab 2013b) and tested on an Intel Core™2 Duo CPU 2.66 GHz, 6 GB RAM. Average computational time for each input set (iteration) was approximately 77 $\mu$s. Although the most relevant papers presenting the MHD algorithms do not mention the time required for computation, the time needed to solve one step calculation can be compared with the results of Lebouvier *et al.*[29] and Rehmet *et al.*[30] in order to demonstrate the difference between computation times. Lebouvier *et al.*[29] utilized MHD models for DC plasma torch. The model was implemented in Code_Saturne software, installed on eight processors (Intel Xeon 2.66 GHz). Each iteration took 54 s on average. Rehmet *et al.*[30] also used MHD modelling for 3-phase plasma torch, with Code_saturne v.2.0 software installed on eight processors (Intel Xeon 2.66 GHz). Each iteration took nearly 80 seconds. Regarding the higher computational speeds and longer computational times in,[26,27] it is obvious that the algorithm proposed in the present paper is fast and computationally undemanding. The reason for this is that the algorithm does not need to solve partial differential equations to predict arc shape, arc voltage, arc velocity and arc energy distribution. For this reason, the algorithm is particularly appropriate to be implemented in broader EAF models with the intent of simulation and model-based control applications due to low computation costs, high accuracy and compatibility with different EAF conditions.

## 4. Conclusion

A computational model and the appropriate algorithm for estimating the distribution of the arc energy dissipation to all three types of heat transfer has been proposed in the present paper. Estimation of the arc energy dissipation is vital in order to determine the optimum manipulated variables in an EAF; however, the literature review shows a lack of suitable arc modules that can be implemented in EAF simulation and control models. The proposed algorithm is based on modified CAM, where the required variables are estimated by using empirical equations and MHD model results.

The application of the model indicated that the functionality of the proposed calculation algorithm is similar to other works that have been reported; however, main advantages of the proposed approach over other algorithms may be summarized as follows: a) simple mathematical background, which leads to significant drop in computational load and consequently short evaluation times in contrast to MHD and Cassie-Mayr models (computational demand is approximately one hundred thousand times lower than comparable MHD models); b) sufficient calculation accuracy (in contrast to the study employing a CAM model,[7] the results are comparable with other similar studies and validated results); c) only two input variables are required, *i.e.* arc length and arc current; d) in contrast to MHD models or CFD models,[31] it does not require a substantial knowledge of processes and information.

For these reasons, the proposed algorithm is suitable for integration into either larger EAF models or into model-based and model-predictive control algorithms, where short calculation time is necessary when it is applied in real time processes.

**Acknowledgment**

The paper received funding from Sharif Research Energy Institute (SERI), project Simulation and control of an EAF. The support of SERI is kindly acknowledged.

## REFERENCES

1) World Steel Association: World Steel in Figures 2012, WSA, Brussels, (2012), 15.
2) R. J. Fruehan, O. Fortini, H. W. Paxton and R. Brindle: Theoretical Minimum Energies to Produce Steel for Selected Conditions, Carnegie Mellon University, Pittsburgh, (2000), 43.
3) J. A. T. Jones: Electric Arc Furnace Steelmaking, American Iron and Steel Institute, Washington DC, (2005), 17, http://www.steel.org, (accessed 2015-01-05).
4) J. L. G. Sanchez, A. N. Conejo and M. A. Ramirez-Argaez: *ISIJ Int.*, **52** (2012), No. 5, 804.
5) F.-H. Wang, Z.-J. Jin and Z.-S. Zhu: *J. Iron Steel Res. Int.*, **13** (2006), No. 5, 7.
6) J. Dai, R. Hao, X. You, H. Sun, X. Huang and Y. Li: 5th IEEE Conf. on Ind. Electronics and Applications, Piacataway, NJ, (2010), 463.
7) J. L. G. Sanchez, M. A. Ramírez-Argaez and A. N. Conejo: *Steel Res. Int.*, **80** (2009), No. 2, 113.
8) S. Arya and B. Bhalja: National Conf. on Recent Trends in Eng. & Technol., BVM Engineering College, Anand, India, (2011), 1.
9) R. Balan, V. Maties, O. Hancu, S. Stan and L. Ciprian: Mediterranean Conf. on Control & Automation, IEEE, Piscataway, NJ, (2007), 1.
10) G. C. Montanari, M. Loggini, A. Cavallini, L. Pitti and D. Zaninelli: *IEEE T. Power Deliver*, **9** (1994), 2026.
11) S. Varadan, E. B. Makram and A. A. Girgis: *IEEE Trans. Power Deliver*, **11** (1996), 1685.
12) Z. Tongxin, E. B. Makram and A. A. Girgis: 8th Int. Conf. on Harmonics and Quality of Power Proc., Vol. 2, IEEE, Piscataway, NJ, (1998), 1079.
13) D. J. Oosthuizen, J. H. Viljoen, I. K. Craig and P. C. Pistorius: *ISIJ Int.*, **41** (2001), No. 4, 399.
14) J. G. Bekker, I. K. Craig and P. C. Pistorius: *ISIJ Int.*, **39** (1999), 23.
15) D. J. Oosthuizen, I. K. Craig and P. C. Pistorius: *Control Eng. Pract.*, **12** (2004), No. 3, 253.
16) J. G. Bekker, I. K. Craig and P. C. Pistorius: *Control Eng. Pract.*, **8** (2000), No. 4, 445.
17) A. Hasannia and H. Esteki: ASME Int. Mechanical Eng. Cong. and Exposition, ASME, Boston, MA, (2008).
18) V. Logar, D. Dovzan and I. Škrjanc: *ISIJ Int.*, **52** (2012), No. 3, 402.
19) V. Logar, D. Dovzan and I. Škrjanc: *ISIJ Int.*, **52** (2012), No. 3, 413.
20) Y. E. M. Ghobara: Master of Applied Science, McMaster University, (2013), 186.
21) A. N. Makarov, Y. A. Lugovoi and R. M. Zuikov: Russian Metall+, **2011** (2011), No. 6, 526.
22) S. Paik and H. D. Nguyen: *Int. J. Heat Mass Trans.*, **38** (1995), No. 7, 1161.
23) R. T. Jones, Q. G. Reynolds and M. J. Alport: *Miner. Eng.*, **15** (2002), No. 11, 985.
24) Q. G. Reynolds: *J. S. Afr. I. Min. Metal.*, **112** (2012), No.7, 605.
25) Q. Reynolds and R. T. Jones: *J. S. Afr. I. Min. Metal.*, **104** (2004), 345.
26) F. Qian, B. Farouk and R. Mutharasan: *Metall Mater. Trans. B*, **26** (1995), No. 5, 1057.
27) Q. G. Reynolds, R. T. Jones and B. D. Reddy: *J. S. Afr. I. Min. Metal.*, **110** (2010), No. 12, 733.
28) P. E. King: Magneto hydrodynamics in Electric Arc Furnace Steelmaking, US Department of the Interior, Bureau of Mines, Pittsburgh, PA, (1990), 24.
29) A. Lebouvier, C. Delalondre, F. Fresnet, V. Boch, V. Rohani, F. Cauneau and L. Fulcheri: *IEEE Trans. Plasma Sci.*, **39** (2011), No. 9, 1889.
30) C. Rehmet, F. Fabry, V.-J. Rohani, F. Cauneau and L. Fulcheri: 21st Int. Symp. on Plasma Chemistry, International Plasma Chemistry Society, Queensland, Australia, (2013), 1.
31) J. C. Gruber, T. Echterhof and H. Pfeifer: *Steel Res. Int.*, **85** (2015), DOI: 10.1002/srin.201400513.